

Circularly-polarized laser-assisted photoionization spectra of argon for attosecond pulse measurements

Z. X. Zhao, Zenghu Chang, X. M. Tong and C. D. Lin

Physics Department, Kansas State University, Manhattan, KS, 66506, USA

zxzhao@phys.ksu.edu

Abstract: Angle-resolved photoelectron spectra of argon atoms by XUV attosecond pulses in the presence of a circularly polarized laser field are calculated to examine their dependence on the duration and the chirp of the attosecond pulses. From the calculated electron spectra, we show how to retrieve the duration and the chirp of the attosecond pulse using genetic algorithm. The method is expected to be used for characterizing the attosecond pulses which are produced by polarization gating of few-cycle left- and right-circularly polarized infrared laser pulses.

© 2005 Optical Society of America

OCIS codes: (320.5550) Pulses; (320.7100) Ultrafast measurements; (260.7200) Ultraviolet, far.

References and links

1. T. Brabec and F. Krausz, "Intense few-cycle laser fields: Frontiers of nonlinear optics," *Rev. Mod. Phys.* **72**, 545–591 (2000).
2. Markus Drescher, Michael Hentschel, Reinhard Kienberger, Gabriel Tempea, Christian Spielmann, Georg A. Reider, Paul B. Corkum, and Ferenc Krausz, "X-ray pulses approaching the attosecond frontier," *Science* **291**, 1923–1927 (2001).
3. M. Hentschel, R. Kienberger, Ch. Spielmann, G. A. Reider, N. Milosevic, T. Brabec, P. Corkum, U. Heinzmann, M. Drescher, and F. Krausz, "Attosecond metrology," *Nature (London)*, **414**, 509–513 (2001).
4. Markus Kitzler, Nenad Milosevic, Armin Scrinzi, Ferenc Krausz, and Thomas Brabec, "Quantum theory of attosecond xuv pulse measurement by laser dressed photoionization," *Phys. Rev. Lett.* **88**, 173904-1–4 (2002).
5. J. Itatani, F. Quéré, G. L. Yudin, M. Yu. Ivanov, F. Krausz, and P. B. Corkum, "Attosecond streak camera," *Phys. Rev. Lett.* **88**, 173903-1–4 (2002).
6. E. Goulielmakis, M. Uiberacker, R. Kienberger, A. Baltuska, V. Yakovlev, A. Scrinzi, Th. Westerwalbesloh, U. Kleineberg, U. Heinzmann, M. Drescher, and F. Krausz, "Direct measurement of light waves," *Science* **305**, 1267–1269 (2004).
7. P. B. Corkum, N. H. Burnett, and M. Y. Ivanov, "Subfemtosecond pulses," *Opt. Lett.* **19**, 1870–1872 (1994).
8. M. Ivanov, P. B. Corkum, T. Zuo, and A. Bandrauk, Routes to control of intense-field atomic polarizability. *Phys. Rev. Lett.* **74**, 2933–2936 (1995).
9. Ph. Antonie, B. Piraux, D. B. Milosevic, and M. Gajda, "Generation of ultrashort pulses of harmonics," *Phys. Rev. A* **54**, R1761-R1764 (1996).
10. V. T. Platonenko and V. V. Strelkov. "Single attosecond soft-x-ray pulse generated with a limited laser beam," *J. Opt. Soc. Am. B* **16**, 435–440 (1999).
11. V. Strelkov, A. Zair, O. Tcherbakoff, R. López-Martens, E. Cormier, E. Mével, and E. Constant, "Generation of attosecond pulses with ellipticity-modulated fundamental," *Appl. Phys. B* **78**, 879–884 (2004).
12. Zenghu Chang, "Single attosecond pulse and xuv supercontinuum in the high-order harmonic plateau," *Phys. Rev. A* **70**, 043802-1–8 (2004).
13. Bing Shan, Shambhu Ghimire, and Zenghu Chang, "Generation of attosecond extreme ultraviolet supercontinuum by a polarization gating," *J. Modern. Optics* **52**, 277–283 (2004).
14. E. S. Toma and H. G. Muller, "Calculation of matrix elements for mixed extreme-ultraviolet-infrared two-photon above-threshold ionization of argon," *J. Phys. B* **35**, 3435–3442 (2002).

15. D. J. Kennedy and S. T. Manson, "Photoionization of the noble gases: Cross sections and angular distributions," *Phys. Rev. A* **5**, 227–247 (1972).
 16. F. A. Parpia, W. R. Johnson, and V. Radojevic, "Application of the relativistic local-density approximation to photoionization of the outer shells of neon, argon, krypton and xenon," *Phys. Rev. A* **29**, 3173–3180 (1984).
 17. M. Y. Adam, P. Morin, and G. Wendin, "Photoelectron satellite spectrum in the region of 3s Cooper minimum of argon," *Phys. Rev. A* **31**, 1426–1433 (1985).
 18. L. V. Keldysh, "Ionization in the field of a strong electromagnetic wave," *Sov. Phys. JETP* **20**, 1307–1314 (1965).
 19. M. Lewenstein, Ph. Balcou, M. Yu. Ivanov, Anne L'Huillier, and P. B. Corkum, "Theory of high-harmonic generation by low frequency laser fields," *Phys. Rev. A* **49**, 2117–2132 (1994).
 20. S. A. Aseyev, Y. Ni, L. J. Frasinski, H. G. Muller, and M. J. J. Vrakking, "Attosecond angle-resolved photoelectron spectroscopy," *Phys. Rev. Lett.* **91**, 223902-1–4 (2003).
 21. R. Trebino, Kenneth W. DeLong, David N. Fittinghoff, John N. Sweetser, Marco A Krumbügel, and Bruce A. Richman, "Measuring ultrashort laser pulses in the time-frequency domain using frequency-resolved optical gating," *Rev. Sci. Instrum.* **68**, 3277–3295 (1997).
-

1. Introduction

Single attosecond extreme ultraviolet (XUV) or soft x-ray pulses can be generated by high-order harmonic generation with few-cycle femtosecond infrared (IR) laser pulses [1]. Due to their short wavelength and weak intensity, conventional autocorrelation method cannot be used to determine their pulse durations directly. So far it has relied on the method of laser-assisted photoionization where photoelectron spectra by XUV pulses are measured in the field of the IR lasers. By varying the time delay between the laser and the XUV pulse, their cross-correlation is built either by laser-induced energy shift [2] or by laser-broadened spectral width [3]. Based on the quantum mechanical formulation of laser-dressed photoionization [4, 5], experimental measurements of photoelectron spectra have been performed and pulse duration of a few hundreds of attoseconds [2] has been determined. Most recently, such technique has also been used to characterize the electric field of a few-cycle laser pulse directly [6]. In the generation and characterization of XUV pulses from these time-resolved measurements, so far only linearly polarized lasers have been used.

An alternative approach to make single attosecond pulses is through the high harmonic generation by the polarization gating method [7, 8, 9, 10, 11, 12]. Using a laser composed of two opposite circular polarizations, it has been demonstrated recently that a supercontinuum covering the plateau and the cutoff region of the harmonic spectrum was generated [13]. How this method works is illustrated in Fig. 1. By superimposing a left-circularly polarized pulse of about 5 fs with a delayed (by about 5 fs) right-circularly polarized pulse, the ellipticity of the combined pulse is shown to reach almost zero over a short time interval near $t=0$ [12]. From Fig. 1, it can be seen that within this interval, for duration of less than an optical cycle, the electric field of one of the two orthogonal components vanishes and the electric field is almost linearly polarized. The radiation generated from such a pulse can be calculated and a supercontinuum spectrum is generated. This supercontinuum is expected to correspond to XUV pulses as short as 200 as. However, this duration has not been determined experimentally as yet. In this paper, we discuss a technique that can be used for measuring the time-dependent electric field of the attosecond pulses. The method employs the cross correlation between the attosecond pulses with the circularly polarized lasers that were used to generate the attosecond pulse.

In such measurements, the attosecond pulse will be delayed by about 5 fs such that the generated photoelectrons only interact with the portion ($t > 5$ fs) of the laser pulse that is almost circularly polarized. To simplify the analysis, we use an ideal circularly polarized field to represent the laser. By refocusing the XUV pulse and the fundamental circularly polarized laser into the argon gas, the XUV pulse characterization will be determined from the measured angle-resolved photoelectron spectra. Such a setup involves XUV photoionization assisted by a short circularly polarized laser. The basic theory for such cross correlation measurement has been

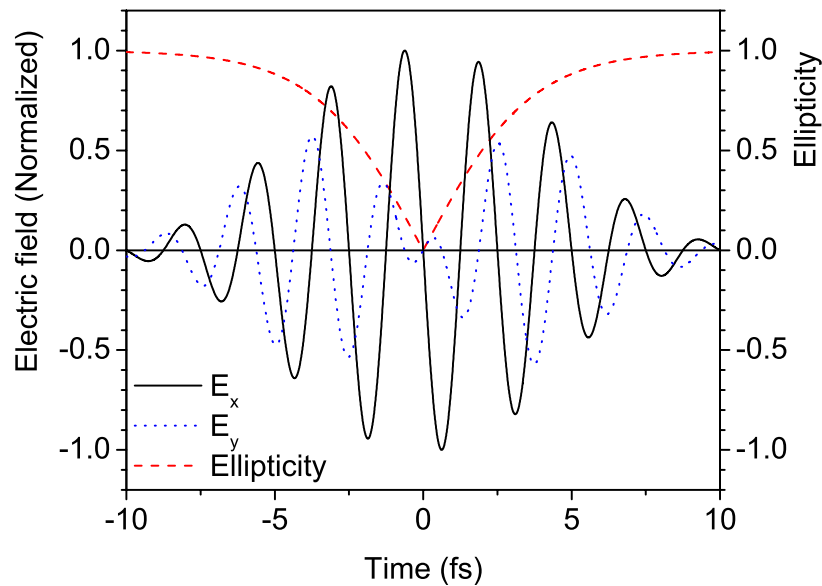


Fig. 1. The time-dependence of the ellipticity and the two perpendicular electric field components of a laser pulse resulting from combining a left-hand circularly polarized pulse and a right-hand circularly polarized pulse. The pulse duration for both circular pulses is 5 fs and the delay between them is 5 fs. The solid and dotted lines represent the two orthogonal field components and the dashed line shows the ellipticity. Note that the small window of vanishing ellipticity or polarization gating where the combined field is nearly linearly polarized.

addressed by Itatani *et al.* [5]. In this paper we examine in detail the laser streaked photoelectron spectra by taking the angle-dependent photoionization cross section into account. We first studied theoretically the angle-resolved photoelectron spectra for such experiments by changing the attosecond pulse parameters, in particular, the pulse duration and the chirp. We illustrate how the electron spectra change with these parameters. From the calculated electron spectra we then showed how to retrieve the attosecond XUV pulse parameters. This technique is expected to be used to determine the attosecond pulses in the time domain when electron spectra from such cross correlation experiments become available.

In Section 2, we address the photoionization of Ar atoms by monochromatic light. The atomic structure parameters from these calculations will be used in Section 3 to generate "theoretical" photoionization electron spectra by attosecond pulses in the presence of circularly polarized lasers. We first explore how the electron spectra change with the pulse duration, and then how they change with the chirp. In Section 4 we discuss how to retrieve the attosecond XUV pulse parameters from the given angle-resolved electron spectra. The last Section gives a short conclusion. Atomic units will be used throughout in this paper unless otherwise indicated.

2. Cross sections and asymmetry parameters for photoionization of Ar

For simplicity we first consider single ionization of Ar atoms by a monochromatic XUV light. We used the single active electron model [14] where the argon atom is described by a model

potential

$$V(r) = -(1 + 5.4e^{-r} + 11.6e^{-3.682r})/r. \quad (1)$$

Starting from the occupied 3p orbital, the electron is released to s-wave or d-wave continuum through one-photon photoabsorption. The radial dipole matrix elements to $\epsilon s (R_-)$ and $\epsilon d (R_+)$ continuum states are given by

$$R_{-(+)} = \int_0^\infty r P_{3p} P_{\epsilon s(\epsilon d)} dr, \quad (2)$$

where the P's are the r-weighted radial wavefunctions. Since there are six 3p valence electrons in the ground state of argon, the total cross section σ_{tot} is proportional to

$$|d|^2 = 6\left(\frac{1}{3}R_-^2 + \frac{2}{3}R_+^2\right) \quad (3)$$

where d is the magnitude of the total transition dipole moment.

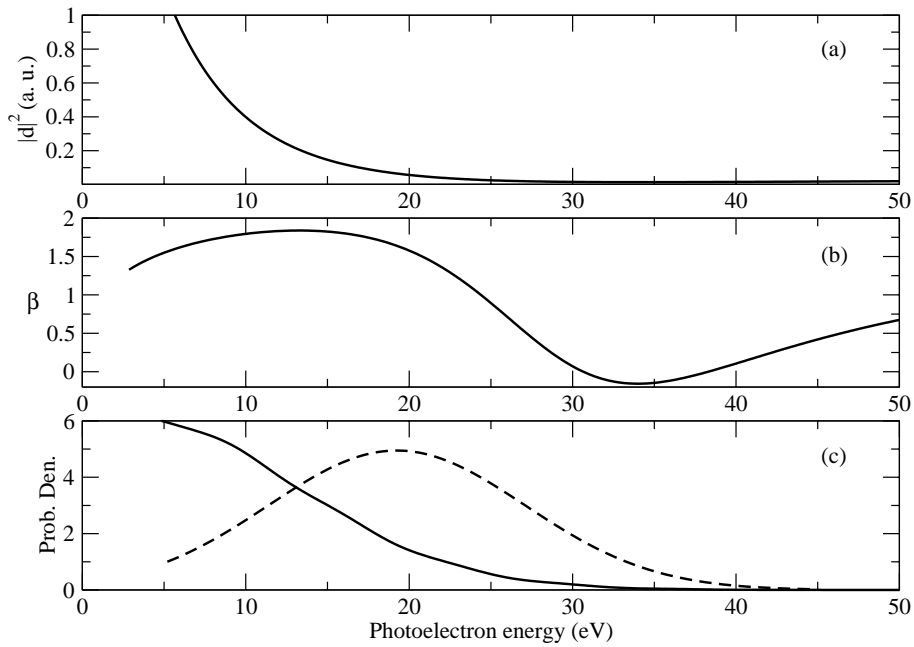


Fig. 2. (a) The square of the dipole transition moment and (b) the asymmetry parameter β from the ground state of Ar by monochromatic light. (c) The ionization probability density vs photoelectron energy of Ar ionized by an XUV pulse which has mean photon energy of 35 eV, duration of 0.1 fs and peak intensity of 10^{12} W/cm². Dashed lines represent the spectral shape of the XUV pulse.

The angular distribution of the photoelectrons by a linearly polarized light is given by

$$\frac{d\sigma}{d\Omega} = \frac{\sigma_{tot}}{4\pi} \left[1 + \beta \frac{3 \cos^2 \theta - 1}{2} \right], \quad (4)$$

where θ is the angle of the electron's final momentum with respect to the light polarization direction, and β is the asymmetry parameter that can be calculated using the method described in [15]. Knowing the β parameter and the total transition dipole moment, in the same spirit

of obtaining differential cross section, we can define an effective angular dependent transition dipole moment for later calculation of laser-assisted photoionization.

Figure 2 shows the calculated (a) $|d|^2$ and (b) the β parameter, versus the photon energy of the monochromatic XUV light. The results from this simple calculation show reasonable good agreement with the more elaborate many-electron calculations [16, 17], including the position of the Cooper minimum. A direct numerical solution of the time-dependent Schrödinger equation for the ionization of argon atom in a short XUV pulse has also been carried out with these pulse parameters: mean photon energy, 35 eV; pulse duration, 100 as; peak intensity, 10^{12} W/cm². The photoelectron spectrum from such calculation is presented in Fig. 2(c). Since the interaction is in the perturbation regime, the spectral intensity distribution of the XUV pulse can be obtained by dividing the electron spectral density by the photoionization cross section, as shown in dashed lines in Fig. 2(c). Under the assumption that the pulse is transform-limited, the XUV pulse in the time-domain is obtained directly by a simple Fourier transformation. However, such an assumption is not valid in general.

3. XUV photoionization assisted by a circularly polarized laser

Let us consider the photoionization of Ar atoms by XUV pulses assisted by a circularly polarized laser field. Electrons that are born at different time within the XUV pulse gain additional time-dependent drift velocity from the laser field which is rotating in time. The XUV pulse with duration τ_x and photon energy ω_x can be generally described by

$$\vec{E}_x(t) = \text{Re}\{E_{0x}e^{-\sigma(1-i\xi)t^2}e^{i\omega_x t}\vec{e}_x\}, \quad (5)$$

where $\sigma = 2\ln 2/\tau_x^2$, and ξ is a dimensionless chirp parameter. The XUV pulse is linearly polarized along x direction with intensity 10^{12} W/cm² and mean photon energy 35 eV. A circularly polarized laser field is characterized by an electric field

$$\vec{E}_l(t) = \frac{1}{\sqrt{2}}E_0(t)[\cos(\omega_l t + \phi)\vec{e}_x + \sin(\omega_l t + \phi)\vec{e}_y] \quad (6)$$

that has a Gaussian shape with FWHM of 5 fs, intensity of 5×10^{13} W/cm². The central wavelength of the laser is taken to be 750 nm.

For electrons born at time t , they gain a drift velocity (proportional to the vector potential of the laser field) given by

$$\vec{v}_l(t) = -\int_{-\infty}^t \vec{E}_l(t) dt. \quad (7)$$

For the convenience of analysis, if the envelope is slow varying, the drift velocity can be approximated by

$$\vec{v}_l(t) \cong \frac{1}{\sqrt{2}\omega_l}E_0(t)[- \sin(\omega_l t + \phi)\vec{e}_x + \cos(\omega_l t + \phi)\vec{e}_y]. \quad (8)$$

According to the strong-field approximation [18, 19], the laser-assisted photoelectron spectrum is given by [4, 5]

$$b(\vec{v}) = i \int_{-\infty}^{\infty} dt d\vec{p}(t) \cdot \vec{E}_x(t) \exp[-i \int_t^{\infty} dt' \frac{[p(t')]^2}{2} + iI_p t] \quad (9)$$

where $b(\vec{v})$ is the amplitude of finding the continuum electron with momentum \vec{v} , $\vec{p}(t) = \vec{v} - \vec{v}_l(t)$ is the instantaneous momentum of electron at time t and I_p is the ionization energy.

From the saddle point analysis, most of the contribution to the time integral comes from the time t_s satisfying the stationary phase condition

$$\frac{1}{2}[\vec{v} - \vec{v}_l(t_s)]^2 = E_0, \quad (10)$$

which is just the classical model used in [2, 3]. It represents energy conservation for photoionization without the presence of lasers, i.e., $E_0 = \omega_x - I_p$. In the calculation, integration over time in Eq. (9) is performed numerically.

3.1. Transform-limited XUV pulses

First we consider transform-limited XUV pulses for which the chirp parameter is zero. XUV pulse parameters are chosen as that used in Fig. 2. Note that the XUV photon energy of 35 eV corresponds to the 21th-order high harmonics from Ti:Sapphire laser field with wavelength 750 nm. Laser intensity was chosen at 5×10^{13} W/cm² such that the ionization probability by the XUV itself (intensity is 10^{12} W/cm²) is two orders higher than that by the laser field. The two pulses peak at the same time $t = 0$. The polarization direction of the XUV pulse is defined as the x-axis (zero angle). The drift velocity at $t = 0$ is along y direction if the laser phase is zero and -x direction if laser phase is $\pi/2$.

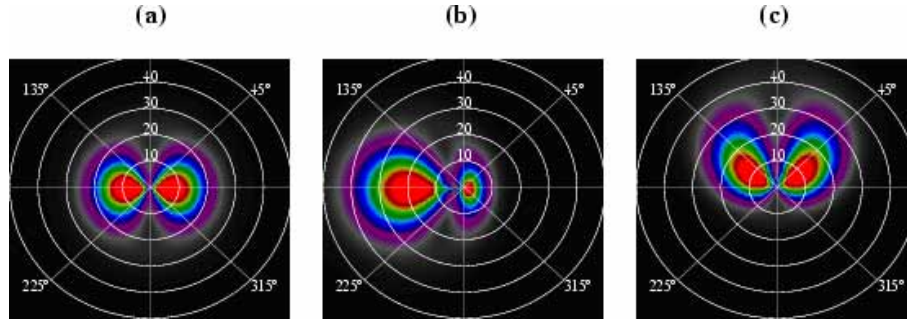


Fig. 3. (a) Energy and angular distributions of photoelectrons from Ar by a single XUV pulse of duration (FWHM) 100 as. The polarization of the XUV pulse is along the x-axis from which the angles of the photoelectrons are measured. (b) and (c), electron spectra by XUV pulses assisted by a circularly polarized laser with phase of $\pi/2$ and 0, respectively. The XUV pulse was assumed to be not chirped.

For XUV photon energy of 35 eV, the asymmetry parameter β is about 1.5, thus the laser-free photoelectrons peak at 0 and 180 degrees as shown in Fig. 3(a). Due to the stronger signal along the XUV polarization direction (x-axis), smaller detection angle is required when the detector is along the x-axis. When a laser field is present, the spectrum is deformed. Fig. 3(b) and Fig. 3(c) show the laser-assisted photoelectron spectra for laser phase of $\pi/2$ and 0, respectively. When the drift velocity is along the $-x$ direction ($\phi = \pi/2$, Fig. 3(b)), more electrons are found in the $-x$ direction and the energy distribution is stretched in the same direction which makes the detection more efficient than the case of laser phase of 0 (Fig. 3(c)). Clearly, phase-stabilized laser of phase $\phi = \pi/2$ is more desirable. In the following, we will only consider laser phase of $\phi = \pi/2$ unless mentioned otherwise.

Figure 4 shows how the electron spectra change with increasing XUV pulse durations. As XUV duration is increased, the energy width of laser-free photoelectron spectra is decreased. On the other hand, when a circularly polarized laser is present, the distribution of the drift velocity that the electrons gain during the XUV pulse duration becomes broader in the angle,

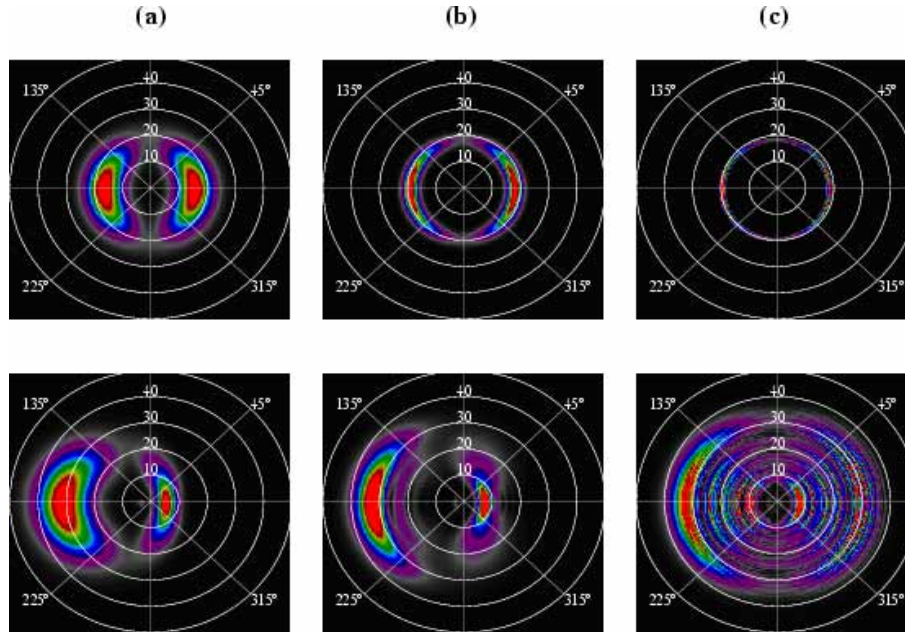


Fig. 4. Dependence of photoelectron spectra on the XUV pulse durations. The upper row is for laser-free photoionization and the lower row is for laser-assisted photoionization where the laser phase was chosen to be $\pi/2$. From (a) to (c) the XUV pulse durations are 0.2, 0.5 and 2 fs, respectively. The XUV pulses are assumed to have no chirp.

thus the resulting photoelectron spectra show broader angular width. When the XUV pulse duration approaches the laser period (Fig. 4(c)), rings-like sideband structures appear following the trajectory of laser's vector potential. The rings-like structures were also observed for linearly polarized laser-assisted photoionization by a train of attosecond pulses [20].

In short, if the XUV pulses are transform-limited, we have:

1. The electron energy width for a given angle decreases as the XUV pulse duration increases.
2. The electron angular width for a given energy becomes broader as XUV pulse duration increases.
3. The electron's momentum image extends in all directions and sideband structure begins to emerge as the XUV pulse duration approaches laser's optical period.

Based on the pulse duration dependence of the spectra, the duration of the attosecond pulse might be deduced by mapping the measured electron velocity image in accordance with the principle of frequency resolved optical gating (FROG) [21]. As suggested by Itatani *et al.* [5], the pulse duration can be retrieved from the angular distribution of electron momentum at a given energy. We will have further discussion on this later.

3.2. Chirp-dependence

In the previous section, we discussed how the electron spectra change with the duration of the XUV pulses when they are transform-limited. However, for transform-limited XUV pulses, the pulse duration can be obtained directly from the bandwidth of the photoelectron energy

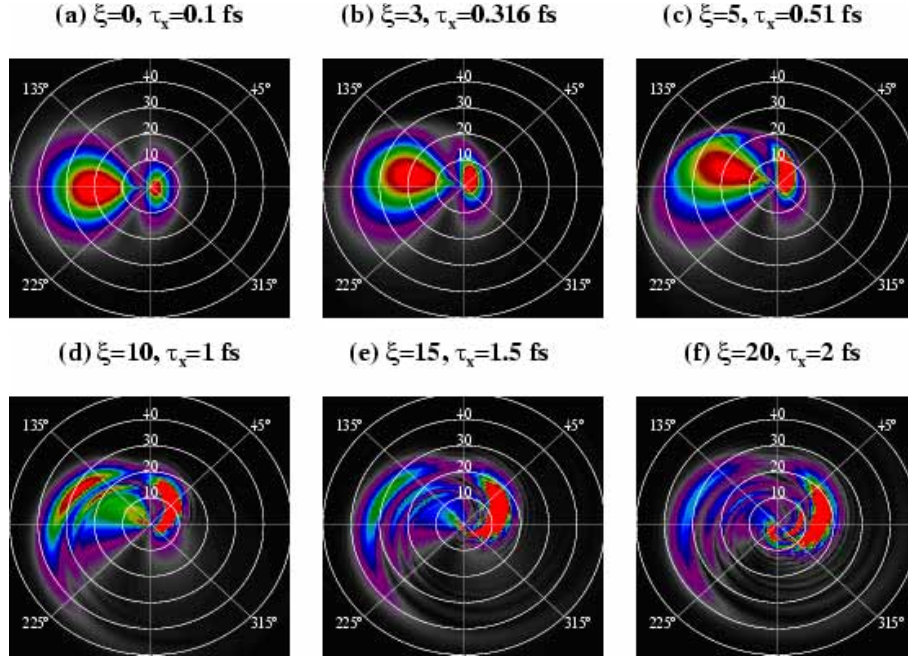


Fig. 5. Photoelectron spectra by laser-assisted XUV pulses with different chirp parameters and pulse durations as indicated in the figure. The frequency width of XUV pulse is fixed as 18.25 eV.

spectrum at any angles, without applying the laser field, as discussed earlier. In general, the chirp parameter of the XUV pulse has to be determined in order to obtain the pulse duration.

For the XUV pulse described in Eq. (5), with nonzero chirp parameter, the frequency bandwidth is given by

$$\Delta\omega = \frac{4\ln 2}{\tau_x} \sqrt{1 + \xi^2}. \quad (11)$$

We will examine laser-assisted electron spectra with fixed frequency bandwidth by varying the pulse duration and the chirp ξ simultaneously. In Fig. 5, we present six cases of chirp parameters and pulse durations: (a) $\xi=0$, $\tau_x=0.1$ fs; (b) $\xi=3$, $\tau_x=0.32$ fs; (c) $\xi=5$, $\tau_x=0.51$ fs; (d) $\xi=10$, $\tau_x=1$ fs; (e) $\xi=15$, $\tau_x=1.51$ fs and (f) $\xi=20$, $\tau_x=2$ fs.

Since the XUV pulse frequency bandwidth is fixed, the laser-free photoionization spectra are the same for all the six cases (see Fig. 3(a)). Thus, the pulse duration can not be resolved by XUV photoionization alone. As the chirp is increased from (b) to (f), the spectral image twists and splashes toward the left (we used left-circularly polarized laser). This behavior can be understood from the modified stationary phase equation (Eq. (10)).

$$\frac{1}{2}[\vec{v} - \vec{v}_l(t)]^2 = E_0 - 2\sigma\xi t = \Omega(t). \quad (12)$$

In contrast to the zero-chirp case, the electron is born with a time-dependent instantaneous energy in a chirped pulse. Thus the final electron momentum is not just rotated by the laser field but also stretched in magnitude due to the chirp. In this case, we can not determine the pulse duration from the angular distribution of the electron momentum at a given energy. Instead, at each angle we can define the center of gravity energy $E(\theta)$ (see Fig. 6). By focusing on this trace for angles larger than 180° , we note that $E(\theta)$ increases monotonically with increasing

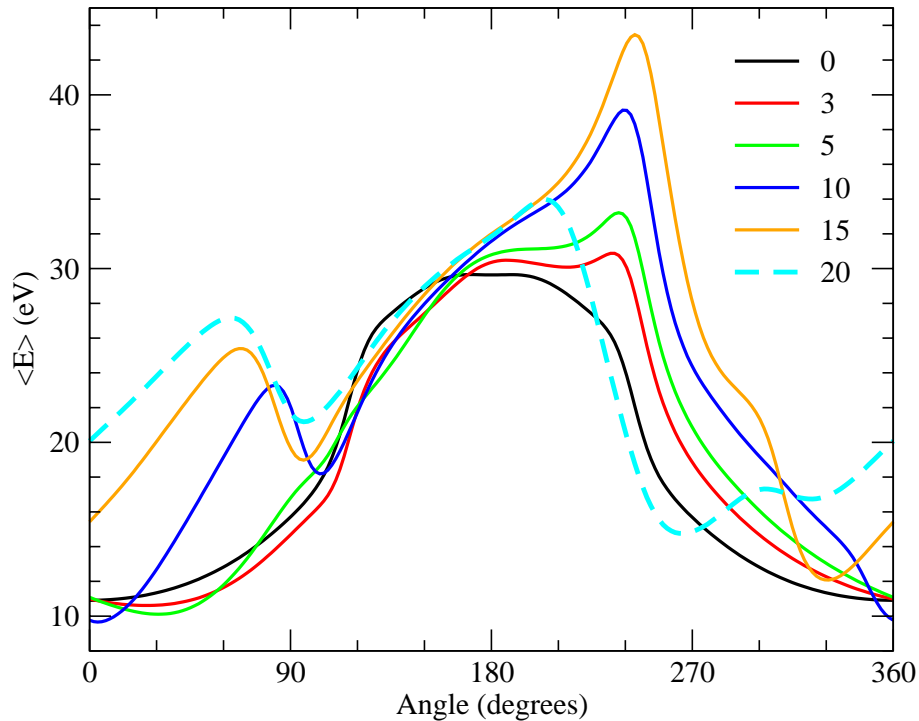


Fig. 6. The center of gravity energy of the photoelectrons vs the electron's angle for different chirp parameters from 0 to 20 of the XUV pulses. The width of the XUV pulse is fixed at 18.25 eV. Note the shift to the higher energy as the chirp parameter increases until at the highest chirp where the pulse duration is close to the optical period.

chirp, until for the large chirp parameter of 20 where the duration of the XUV pulse of 2.0 fs is close to the laser period. This trace, combining with the angular width, qualitatively illustrate the chirp and pulse duration dependence of the XUV pulses in the time-domain.

3.3. Double XUV pulses

Next we consider a pulse train consisting of double pulses without chirp, separated by $T_0/2$ (i.e., one half of the laser period),

$$E_x(t - T_0/4) + E_x(t + T_0/4). \quad (13)$$

Each pulse has a duration of 0.2 fs and corresponding peak intensity 10^{12} W/cm². When the polarization gating is not short enough, such a train of two attosecond pulses are generated.

For such a pulse train, the laser-free photoelectron energy spectra consist of two rings separated by $2\omega_l$, see Fig. 7(a). When the laser field is present, the spectra is distorted but are made of two identical pairs. In Fig. 7, the laser phases are $0, \pi/4, \pi/2$, respectively, from (b) to (d). In (b) electrons generated by the left pulse experience a $+x$ shift, while electrons generated by the right pulse experience a $-x$ shift. Thus the total electron spectra are stretched along the x -axis. In (c), electrons generated by the two pulses shift about half way toward the 45 degrees (and 225 degrees) line. In (d), the shifting to this diagonal line is complete and the electron spectrum shows a butterfly shape.

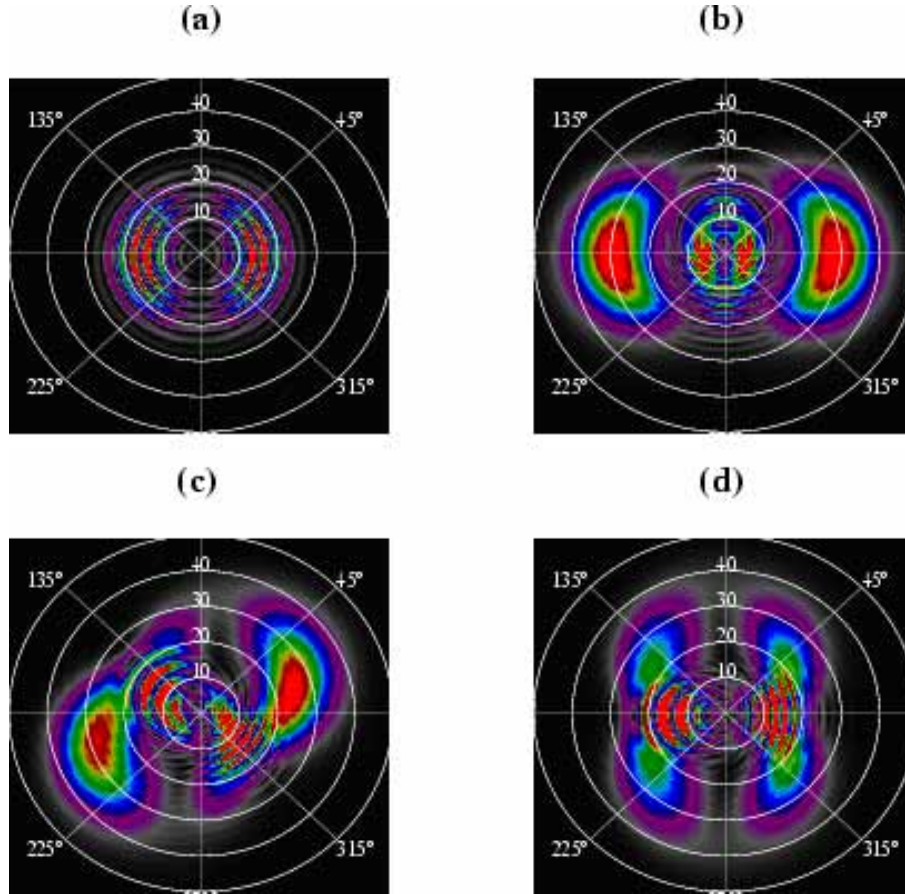


Fig. 7. Photoelectron spectra by a train of two attosecond XUV pulses: (a) no laser ; (b),(c),(d), with lasers, of phase 0, $\pi/4$ and $\pi/2$, respectively.

4. Retrieving the XUV pulse information

The laser-free photoionization spectrum is obtained from this equation

$$b(\vec{v}) = i \int_{-\infty}^{\infty} dt \vec{d}(\vec{v}) \cdot \vec{E}_x(t) \exp[i(1/2)v^2 t + iU_p t]. \quad (14)$$

If both the magnitude and phase of the photoelectron spectrum are known, the pulse information can be retrieved directly by inverse Fourier transformation. However, only $|b(\vec{v})|^2$ is available experimentally. In order to obtain the phase information, one has to rely on the additional information supplemented by the laser-assisted photoionization measurement which builds the cross-correlation between the XUV pulse and the laser pulse. Our procedure of retrieving the XUV pulse can be described as follows: 1) using the measured laser-free spectra as input; 2) starting with a simple guess of the phase of $b(\vec{v})$ to reconstruct the XUV pulse; 3) use the guessed XUV pulse to calculate laser-assisted photoelectron spectra; 4) compare the calculated spectra with the measured spectra and the discrepancy is recorded as the error function; 5) repeat processes 2) to 4) with another guess until best fitting is found.

This fitting process can be improved by using genetic algorithm. To speed up the retrieving process, instead of comparing the 2D momentum image, we compare only the trace $E(\theta)$ de-

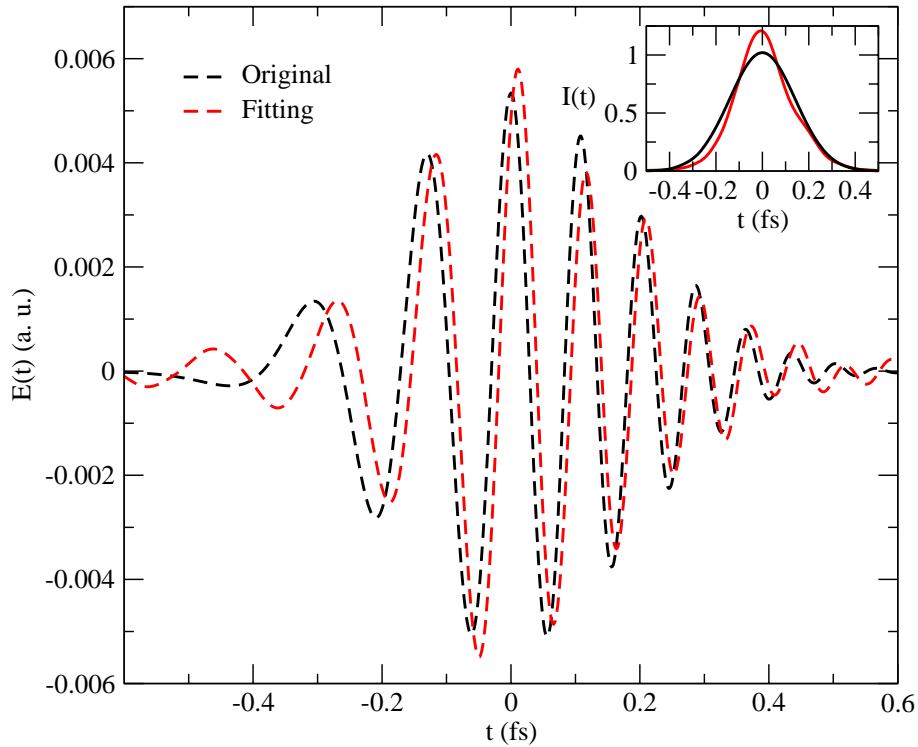


Fig. 8. Comparison of the retrieved electric field with the original field. The inset shows the intensity profile of the original and the retrieved pulses, in units of 10^{12}W/cm^2 .

defined earlier. In the simplest case, if we assume the XUV pulse has a Gaussian profile and is linearly chirped, then only one parameter needs to be fitted based on Eq. (11).

For the general pulse shape and chirp, we can either discretize the phase into N slices and varying them independently to find the best fit, or expand the phase into a polynomial

$$\phi(\omega) = \sum_{i=1}^N c_i (\omega - \omega_0)^i \quad (15)$$

where ω_0 is the center frequency, and the second order term corresponds to the linear chirp of the pulse. Our simulation shows that the latter method converges faster and is indeed used to retrieve the pulse information in the following example.

To illustrate the retrieving method, we assume that the measured photoelectron spectrum is given as in Fig. 5(b). We used the procedure described above to retrieve the XUV pulse information. In the simulation, we chose $N=5$. The retrieved pulse is compared to the original pulse in Fig. 8. Good agreement can be seen in both the magnitude and the phase of the retrieved electric field. The agreement in the intensity profile is also quite good as seen in the inset. As a further check on how well the retrieved pulse agrees with the original one, we also simulate the electron spectrum at time delay of -0.2 fs using both the original and the retrieved pulses where the first spectrum was supposedly determined experimentally. As shown in Fig. 9, the two spectra are in reasonable good agreement with each other.

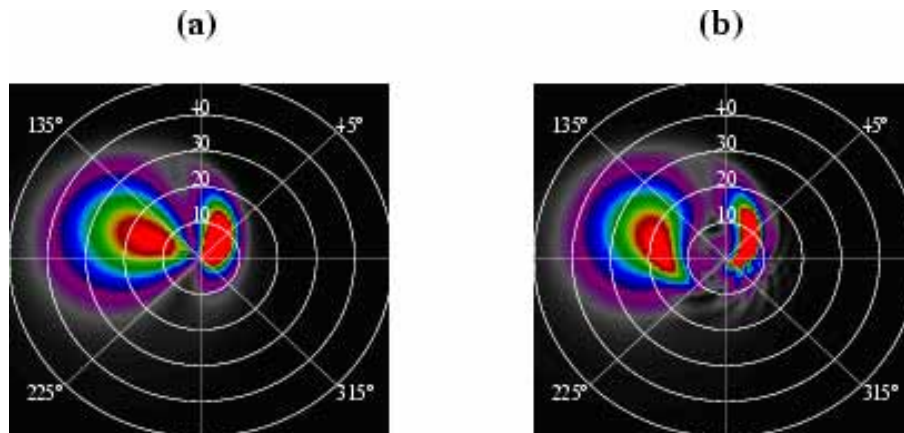


Fig. 9. Comparison of the photoelectron spectra calculated using (a) the original pulse and (b) the retrieved pulse, at a different time delay of -0.2 fs.

5. Summary and conclusion

In summary, we have performed calculations of angle-resolved photoelectron spectra of Ar atoms in the combined field of an attosecond XUV pulse and a circularly polarized laser pulse. We examined first theoretically how the electron spectra, including the angular distributions, depend on the pulse duration and the chirp parameter of the XUV light pulse. We also showed how to retrieve or measure the pulse duration and the chirp parameter of such an attosecond XUV pulse if the angle-resolved electron spectra are available from experiments. The method requires that the few-cycle lasers be well characterized already, including its carrier envelope phase.

By focusing on the main features of the laser-assisted photoelectron spectra such as the mean kinetic energy of the photoelectron at a given angle, we showed that it is possible to retrieve the pulse duration and the chirp parameter from the measured electron energy and angular distributions at a given time delay. Systematic check can be further made through multiple measurements by varying the time delay between the XUV and IR pulses. For attosecond XUV pulses generated by the polarization gating method, the procedure presented in this paper is expected to be used to characterize the pulse when photoelectron spectra from such cross-correlation measurements become available.

Acknowledgments

This work is in part supported by Chemical Sciences, Geosciences and Biosciences Division, Office of Basic Energy Sciences, Office of Science, U.S. Department of Energy.